Journal of Hazardous Materials 186 (2011) 1681–1686

Contents lists available at ScienceDirect

Journal of Hazardous Materials

journal homepage: www.elsevier.com/locate/jhazmat

Adsorption–desorption properties and characterization of crosslinked Konjac glucomannan-graft-polyacrylamide-co-sodium xanthate

Lu-Feng Wang, Jia-Cai Duan, Wen-Hua Miao, Ruo-Jie Zhang, Si-Yi Pan, Xiao-Yun Xu*

College of Food Science and Technology, Huazhong Agricultural University, No.1, Shizishan Street, Wuhan, Hubei 430070, China

ARTICLE INFO

Article history:
Received 3 August 2010
Received in revised form
10 December 2010
Accepted 13 December 2010
Available online 21 December 2010

Keywords:
Konjac
Flocculant
Adsorption
Regeneration
Characterization

ABSTRACT

A new flocculant, based on Konjac-graft-poly (acrylamide)-co-sodium xanthate (CKAX), was synthesized in aqueous solution using epichlorohydrin (ECH) as the cross-linker and ceric ammonium nitrate (CAN) as the initiator. X-ray diffraction indicated the existence of strong interaction between KGM and reactant, including intermolecular and intramolecular hydrogen bonds. Microscopy images exhibited the appropriate pore size and distribution, which might be related to a higher capacity of flocculation and adsorption. Thermo gravimetric analysis showed that the synthetic polymer could improve the thermo-stability of the natural polysaccharides, and there was a positive correlation between polymer residual weight and flocculation. The adsorption and desorption properties for copper ions indicated that the adsorption rate could be described by a pseudo-second-order rate model, and the Freundlich model provides the best fit for the resulting adsorption isotherm. The flocculant can be regenerated in HNO_3 solution.

1. Introduction

Today, the emphasis on synthetic chemical use is based on screening new strains producing highly efficient and cost-effective flocculants [1–4]. Synthetic organic polymers have some advantages, such as inertness to pH changes, formation of large cohesive flocs and versatile tailor ability [5]. In comparison with organic flocculants, inorganic flocculants which are usually salts of multivalent metals, like aluminium or iron, normally require greater dosage and are more pH sensitivity [6]. Therefore, obtaining new materials with desirable properties of both the chemical combination of natural and synthetic polymers could be a feasible way to improve the flocculating activity and reduce the cost.

Chemical grafting is one of the most effective methods of modifying the structure and properties of polymers and it has been reported that graft copolymerization has largely retrenched the industry cost and improved the functional properties of natural polysaccharides [7,8]. Currently in the field of flocculants, a great deal of attention has been directed towards the preparation of Konjac glucomannan (KGM)-based composites [9–13].

KGM is a water-soluble non-ionic polysaccharide extracted from tubers of the Amorphophallus Konjac plant, and it consists of 1,4-linked-β-D-mannopyranose and β-D-glucopyranose units in a molar ratio of 1.6:1 [14] with a low degree of acetyl groups (approximately 1 acetyl group per 17 residues) at the side chain C-6 position [15,16]. Moreover, KGM is a renewable and biodegradable natural polysaccharide with a large number of hydrophilic –OH groups, which makes KGM a better raw material as an adsorbing agent [17].

There are some reports in the literature on the modification of KGM [18–20], and Xie et al. [21] recently reported on a flocculant from phosphate etherification of KGM. However the synthesis on the basis of KGM, with the dual function of trapping dissolved heavy metal ions and removing suspended particle in aqueous solution, has not yet been reported.

In this article, a novel flocculant was synthesized by introducing PAM graft chains and xanthogenation with strong ligands. This dual flocculant has tremendous potential use in the wastewater treatment industry, not only in removing dissociative metal ions, but also in reducing the components causing turbidity in water. In this study, the polymer was characterized by XRD, SEM and TGA; the adsorption and desorption properties for copper ions were investigated, as well as the regeneration of CKAX.

2. Materials and methods

2.1. Materials

The Konjac powder was provided by Enshi Konjac Factory, Hubei, China. The acrylamide (AM, chemically pure) was supplied by Sinopharm Chemical Reagent Co., Ltd., Shanghai, China, and the ceric ammonium nitrate (CAN) by Tianjin Chemical Reagent Co., Ltd., Tianjin, China. The epichlorohydrin and carbon disulfide were

* Corresponding author. Tel.: +86 27 87671056; fax: +86 27 87288373.
E-mail address: xiaoyunxu88@gmail.com (X.-Y. Xu).

0304-3894/$ – see front matter © 2010 Elsevier B.V. All rights reserved.
doi:10.1016/j.jhazmat.2010.12.055

from Wuhan Organic Chemistry Reagent Factory, Wuhan, China. Kaolin (2%) and $CuCl_2$ solution (1000 mg/L) were prepared as stock solutions. The ceric ammonium nitrate (CAN) was purchased from Sigma–Aldrich. Other reagents were used as purchased. All the solutions in the experiment were prepared with distilled water.

2.2. Preparation of crosslinked Konjac glucomannan-graft-Poly (acrylamide)-co-sodium xanthate (CKAX) [22–24].

A series of reagents with different amounts of Konjac powder, crosslinker, initiator, ceric ammonium nitrate and acrylamide were prepared by the following procedure: Konjac powder of different amounts and distilled water were placed in a 500 mL three-necked flask equipped with a stirrer, a condenser, and a nitrogen line, and then thoroughly mixed. The slurry was heated to 35 °C, and the temperature was maintained in a water bath. Epichlorohydrin was added dropwise with slow stirring. This process of crosslinking was allowed to react at 35 °C for 2 h. The slurry was then heated to 45 °C for 30 min under nitrogen atmosphere. A quantitative volume of CAN (dissolved in 1 mol/L nitric acid) was added into the flask. The reaction was continued for 15 min. After AM solutions were added, the grafting polymerization process was maintained at 45 °C for 2.5 h. Then the slurry was quickly cooled to 30 °C and the nitrogen flow was stopped. A certain amount of NaOH solution and CS_2 was slowly added into slurry for xanthating and the reaction was carried out at 30 °C for 2 h. The color turned to saffron yellow. The product was washed successively with anhydrous ethanol at room temperature, dried in a vacuum oven at 60 °C to a constant weight, and then was milled and screened. The samples for experimental use had a particle size in the range of 40–80 mesh.

2.3. Characterization

2.3.1. X-ray diffraction (XRD)

X-ray diffraction of the films was analyzed using a Shimadzu XRD-6000 (Japan) diffractometer equipped with a Cu Kα target at 40 kV and 30 mA with a scan rate of 4°/min. The diffraction angle ranged from 10° to 50°.

2.3.2. Scanning electron microscope (SEM)

Surface morphological structure of KGM and polymers in powdered form was analyzed in a scanning electron microscope. The samples were sprayed with gold under vacuum and a magnification of 2000–8000 times was obtained.

2.3.3. Thermal gravimetric analysis (TGA)

Thermal gravimetric measurements were performed using Netzsch STA 449C instrument (Germany) under a nitrogen atmosphere with a flow capacity of 30 mL/min. The scan was carried out at a heating rate of 10 °C/min from 30 to 400 °C. The sample weight of approximately 8–10 mg was analyzed using an $-Al_2O_3$ crucible.

2.4. Adsorption experiments

CKAX (0.05 g) was added to a 250 mL beaker containing 100 mg/L of $CuCl_2$ solution (100 mL). The pH was prior adjusted to 5.0 using hydrochloric acid solution (1.0N). The mixture was stirred for different times (2–80 min) at 25 °C. The amount of copper ions adsorbed on the CKAX at adsorption equilibrium was calculated according to the following equation (1):

$$Q_e = V\frac{C_0 - C_e}{W} \quad (1)$$

where C_0 and C_e are the initial and equilibrium copper ions concentrations (mg/L), respectively; V is the volume of the solution (L) and W is the weight of the CKAX used (g).

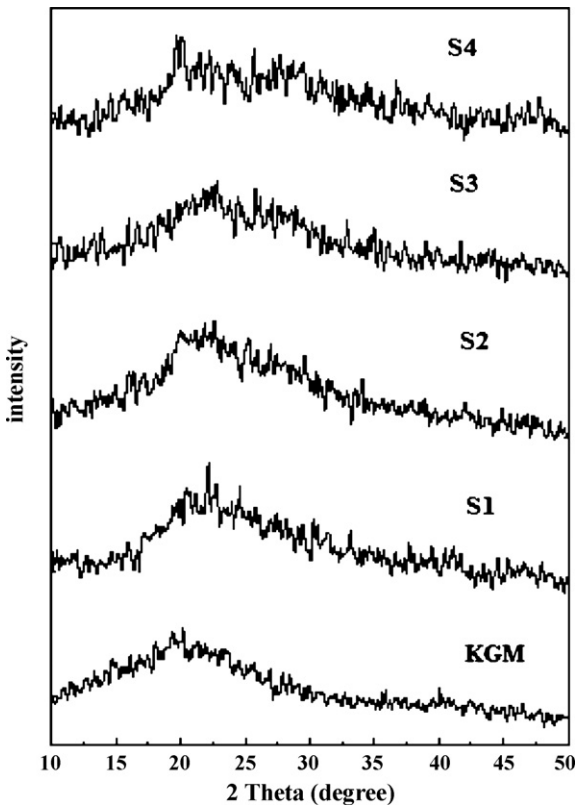

Fig. 1. X-ray diffraction patterns of KGM and modified KGM samples.

2.5. Regeneration of CKAX

HCl and HNO_3 solutions (0.2 mol/L) were used as desorption media for CKAX regeneration. The CKAX was added to 100 mL of the desorption solution after the first equilibration settled in a solution with an initial concentration of 100 mg/L copper ions at pH 5.0. After stirring at a speed of 150 rpm for 30 min in order to facilitate desorption, the CKAX was then moved to deionized water for thorough washing for preparation for further trial runs. The concentration of copper ions of desorption solution was examined. The adsorption–desorption experiments were conducted using 4 cycles. The removal rate of copper ions (Hr) was calculated as equation (2), and the desorption ratio (D) was calculated as equation (3) below:

$$\mathrm{Hr} = \frac{C_0 - C_1}{C_0} \times 100\% \quad (2)$$

$$D = \frac{C_2}{C_0 - C_1} \times 100\% \quad (3)$$

where Hr is the removal rate of copper ions (%), D is the desorption efficiency (%), C_0 and C_1 are the copper ion concentrations of the initial suspension and supernatant (mg/L), respectively, C_2 is the concentration of desorption solution (mg/L).

3. Results and discussion

3.1. Wide angle X-ray diffractometry

Wide angle X-ray diffractometry (XRD) was used to probe the crystal behavior of the samples. The XRD patterns of KGM and the modified KGM are displayed in Fig. 1. The XRD patterns of the neat KGM displays a typical broad hump located around $2\theta = 20°$ with ill-defined diffraction peaks, which indicates that the neat KGM is in the amorphous phase [25]. Several small and weak crystalline peaks

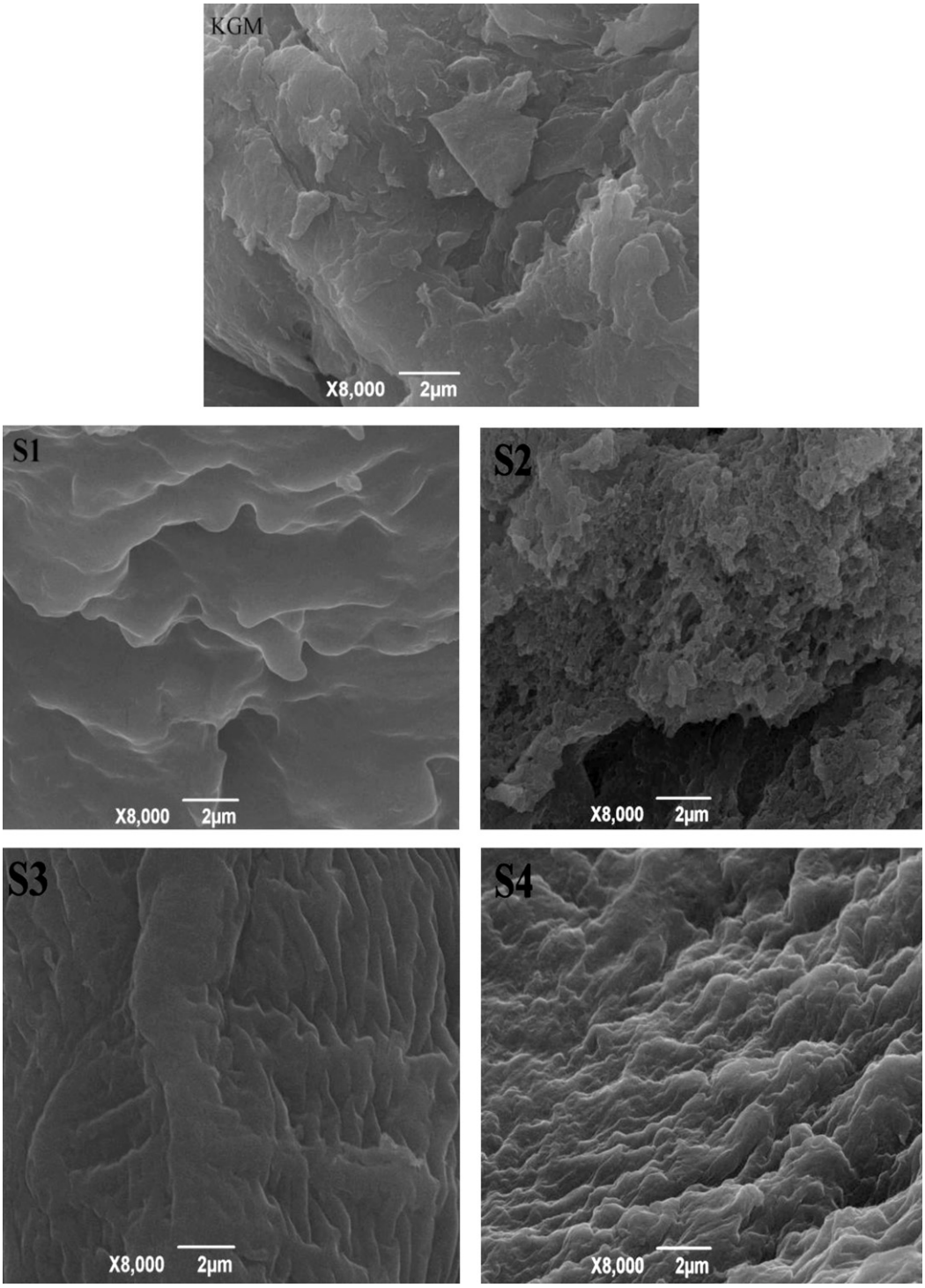

Fig. 2. SEM images of KGM and modified KGM samples.

at 15°, 36°, and 40°, were assigned to a few Mannan II crystals of KGM glucomannan [26]. The broad hump at about $2\theta = 20°$ gradually split into two small separate humps with an increase of copper ion removal rate from 67% to 95%. According to Mishra et al. [27], the XRD pattern of polyacrylamide is quite broad, representing relatively small sized crystals of the polymer. The results in this study indicated that strong interactions exist between KGM and reactant, including intermolecular and intramolecular hydrogen bond interactions.

3.2. Surface morphology

The surface morphology of KGM and samples provides insight into the structural information of the products, as exhibited in Fig. 2. The relative smooth structure of KGM was converted to the alveolate structure after modification. However, the SEM photographs of samples showed variability in the size and the distribution of the pores, which were invariably formed due to the different degree of reaction. For instance, the pores of S1 are too large and dispersed,

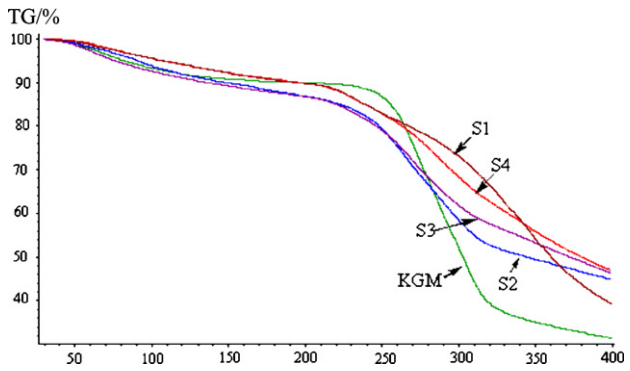

Fig. 3. TGA curves of KGM and modified samples.

while that of S4 are too small and dense compared with S2 and S3. The products of appropriate pore size and distribution will possess relatively higher capacity of flocculation and adsorption. It is suggested that; if the pore is too large, it will weaken its persistence capacity of flocculation and adsorption; while an uneven surface with excess small pores (due to the excessive degree of reaction), will increase the difficulty of particles and heavy metal ions in combining with the flocculants.

3.3. Thermo gravimetric analysis

The thermo gravimetric analysis curves of different samples are shown in Fig. 3. All the samples had a weight loss of about 10% in the range of 30–120 °C, owning to the release of water molecules from the samples. Pure KGM shows a one stage decomposition process within the range of 230–360 °C, characterized by a weight loss of about 56%. The data is consistent with reported literature about KGM and maybe attributed to the loss of hydroxyl groups of KGM from water molecules and disintegration of macromolecule chains of KGM [28]. Moreover, with increased temperature, the maximum weight loss of most of the samples appears in the range of 210–370 °C, corresponding to the decomposition of samples. The experiment was carried out under similar conditions to the previous reports and results are homologous [25–27].

The relative thermal stability of each sample was evaluated by comparing the residual weight percent at final temperature. According to Table 1, pure KGM showed a residual weight percent of 31.4% at 400 °C. However, the residual weight percent (39.1%, 44.8%, 46.3%, 46.9%) of all modified samples at 400 °C is higher than that of the pure KGM, which indicates the presence of strong interactions of amide groups of PAM, xanthogenic groups and the hydroxyl groups of KGM [26]. Furthermore, the Cu^{2+} ions and turbidity removal rate from samples are correlated with their thermal properties. There is a higher removal rate of Cu^{2+} ions corresponding to higher residual weight at 400 °C, which may be connected with the interactions mentioned. The observed data implies that the synthetic polymer could improve the thermo-stability of the natural polysaccharides.

Table 1
The residual weight of KGM and modified KGM samples.

Sample	Degradation stage	Temperature range (°C)	Weight loss (%)	Residual weight at 400°C (%)	Hr (%)
KGM	1	30.8–150.1	10.2	31.4	35.7
	2	210.7–370.6	56.4		
S1	1	32.3–150.8	7.9	39.1	67.3
	2	210.5–370.5	42.8		
S2	1	29.7–150.1	9.3	44.8	78.2
	2	210.8–370.5	38.7		
S3	1	31.1–150.6	10.9	46.3	87.4
	2	210.7–370.5	37.4		
S4	1	31.8–150.1	7.8	46.9	95.7
	2	210.4–370.6	35.8		

3.4. Adsorption kinetics

Several kinetic models were used to analyze the experimental data in order to determine the mechanism of the adsorption process. By integrating the pseudo-first-order equation and the pseudo-second-order equation at the boundary condition of $Q_t = 0$ at $t = 0$ and $Q_t = Q_t$ at time t, new equations result:

$$\ln(Q_e - Q_t) = \ln Q_e - k_1 t \quad (4)$$

$$\frac{t}{Q_t} = \frac{1}{k_2 Q_e^2} + \frac{1}{Q_e} t \quad (5)$$

where Q_t is the amount adsorbed on the adsorbent at time t; k_1 is the rate constant of pseudo-first-order; Q_e denotes the amount of adsorption at equilibrium; k_2 is the rate constant of pseudo-second-order adsorption.

The intraparticle diffusion equation is:

$$Q_t = k_i t^{0.5} + C \quad (6)$$

where k_i is the intraparticle diffusion rate constant, C is regression constant.

The plots of $\ln(Q_e - Q_t)$ versus t, t/Q versus t and Q_t versus $t^{0.5}$ are shown in Fig. 4(a, b and c, respectively). The values of Q_e, k_1, and k_2 can be calculated from the slopes and the intercepts of the straight lines and the data is presented in Table 2.

As shown in Table 1, the second-order equation ($R^2 = 0.999$) described the experimental data more accurately in comparison with the first-order equation ($R^2 = 0.919$) in consideration of equilibrium sorption capacities and correlation coefficients. The first-order kinetic process was used for reversible reaction with an equilibrium being established between liquid and solid phases. Whereas, the second-order kinetic model assumes that the rate-limiting step may be chemical adsorption. According to Table 1, the adsorption data did not fit the intraparticle diffusion equation ($R^2 = 0.887$). The above results indicated that the adsorption process is controlled by two or more rate-limiting steps, such as external diffusion, boundary layer diffusion and intraparticle diffusion.

3.5. Adsorption isotherms

Adsorption isotherm is very important to describe how solutes interact with the adsorbent. The Langmuir and Freundlich equations are often used to describe equilibrium sorption isotherms because of their relative simplicity and reasonable accuracy [29]. The Langmuir equation can be best used to describe a monolayer adsorption, whereas the Freundlich equation can be used to describe a monolayer adsorption as well as a multilayer adsorption [30].

The equilibrium adsorption of Cu^{2+} on CKAX as a function of the initial concentration of Cu^{2+} at 298 K, 308 K and 318 K is shown in Fig. 5. The plots of C_e/Q_e versus C_e and $\ln Q_e$ versus $\ln C_e$ are shown

Table 2
Adsorption kinetics parameters for Cu^{2+} on CKAX.

Kinetics model	Parameters		
Pseudo-first-order	Q_e (mg/g)	k_1 (min^{-1})	R^2
	91.5	0.958	0.919
Pseudo-second-order	Q_e (mg/g)	k_2 (g/mg min)	R^2
	92.6	0.0142	0.999
Intraparticle diffusion	C	k_i (mg/g $h^{0.5}$)	R^2
	81.5	1.92	0.887

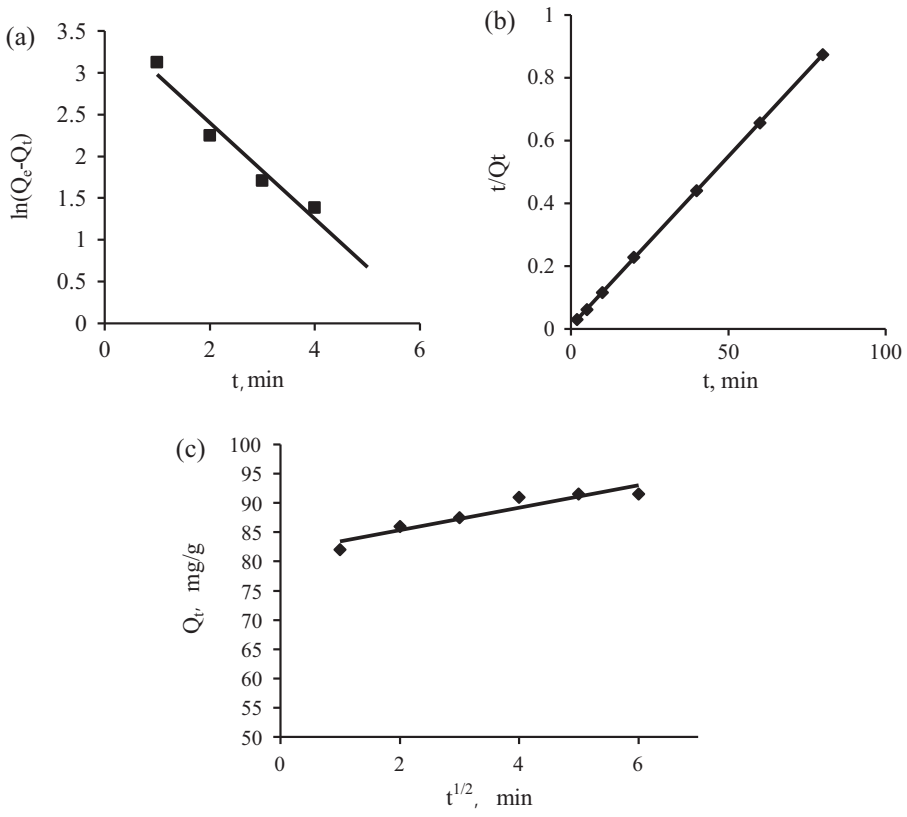

Fig. 4. Plot of the pseudo-first-order (a), pseudo-second-order (b) and intraparticle diffusion (c).

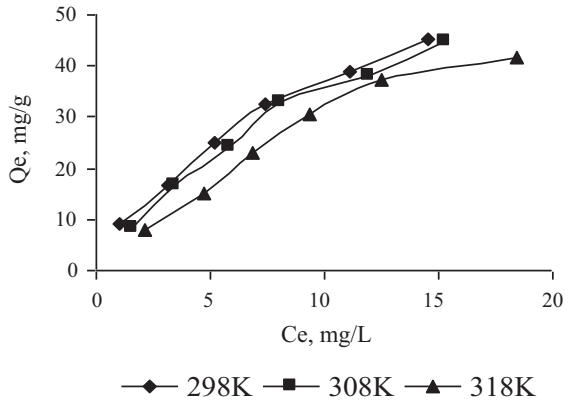

Fig. 5. Adsorption isotherm of Cu^{2+} on CKAX.

in Fig. 6(a and b, respectively). The model parameters and correlation factor (R^2) are listed in Table 3. Both Langmuir and Freundlich equations can describe the adsorption behavior of copper ions on CKAX according to the parameters in Table 3. However, the Freundlich model gives a better fit to the experimental data than the Langmuir model because the correlation coefficient of Freundlich equation was higher than that of Langmuir equation at different temperatures. The K_L and K_f decreased with an increase of temperature, indicating that the adsorption behavior is an exothermic process. In the Freundlich model, favorable adsorption occurs when the n value is above 1. The n values in Table 3 were all above 1, indicating that the CKAX is useful in the adsorption of copper ions.

3.6. Regeneration of CKAX

It is important to examine the possibility of desorbing the copper ions adsorbed on CKAX and reusing them for potential

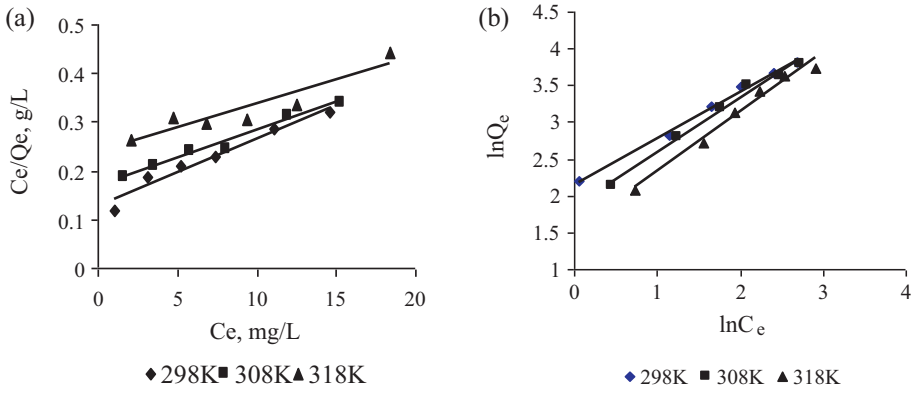

Fig. 6. Langmuir isotherm (a) and Freundlich isotherm (b).

Table 3
Adsorption isotherm parameters for Cu^{2+} on CKAX.

	Temperature (K)	Q_m (mg/g)	K_L	R^2
Langmuir	298	71.43	0.111	0.959
	308	87.72	0.0680	0.977
	318	102.0	0.0410	0.864
	Temperature (K)	n	K_f	R^2
Freundlich	298	1.581	8.58	0.995
	308	1.358	6.42	0.988
	318	1.238	4.56	0.978

Table 4
Effect of regeneration on the ability CKAX.

Cycle time	HCl solution		HNO_3 solution	
	Hr (%)	D (%)	Hr (%)	D (%)
1	86.5	96.2	87.4	97.3
2	80.3	87.4	82.1	90.2
3	72.1	78.5	72.3	82.6
4	54.7	56.6	64.5	70.8

practical application [31,32]. The corresponding desorption efficiencies obtained using HCl and HNO_3 solutions are shown in Table 4. The desorption efficiency reached about 96% and the removal rate of copper ions was above 86% after the first cycle, which indicated that there were no obvious differences between the CKAX and desorbed CKAX after the first cycle. After four cycles of adsorption–desorption, the adsorption and desorption efficiency was also above 50%, which showed excellent desorption properties of the new material. From Table 4, Hr and D values in HNO_3 were always higher than in HCl solution in the four cycles. We can conclude that HNO_3 is more effective than HCl in the regeneration test.

4. Conclusions

CKAX was synthesized and characterized by XRD, SEM and TGA. XRD demonstrated that KGM showed an amorphous structure with only a few crystals. After modification, crystal structure of the samples had no visible change, but some new diffraction peaks appeared, and the peak intensity of CKAX decreased significantly with the surface spacing became smaller. TGA displayed that the higher the residual weight of sample, the better the adsorption ability. SEM indicated that the size of hole on the sample surface could affect adsorption, with extreme small or large holes not suitable for adsorption. The adsorption–desorption experiments showed that the adsorption rate could be described by pseudo-second-order rate model, and the Freundlich model provides a better fit for the adsorption isotherm. The adsorbent can regenerate in HNO_3 solutions.

Acknowledgment

This work was partly supported by the National Natural Science Foundation of China (Grant No. 30972044).

References

[1] B.Y. Gao, Q.Y. Yue, Y. Wang, W.Z. Zhou, Color removal from dye-containing wastewater by magnesium chloride, J. Environ. Manage. 82 (2007) 167–172.
[2] B.Y. Gao, Y. Wang, Q.Y. Yue, J.C. Wei, Q. Li, Color removal from simulated dye water and actual textile wastewater using a composite coagulant prepared by polyferric chloride and polydimethyldiallylammonium chloride, Sep. Purif. Technol. 54 (2007) 157–163.
[3] B.Y. Gao, Q.Y. Yue, Y. Wang, Coagulation performance of polyaluminum silicate chloride (PASiC) for water and waste water treatment, Sep. Purif. Technol. 56 (2007) 225–230.
[4] B.Y. Gao, Y. Wang, Q.Y. Yue, J.C. Wei, Q. Li, The size and coagulation behavior of a novel composite in organic-organic coagulant, Sep. Purif. Technol. 62 (2008) 546–552.
[5] R.P. Singh, B.R. Nayak, D.R. Biswal, T. Tripathy, K. Banik, Biobased polymeric flocculants for industrial effluent treatment, Mater. Res. Innovations 7 (2003) 331–340.
[6] S.K. Rath, R.P. Singh, Flocculation characteristics of grafted and ungrafted starch, amylose, and amylopectin, J. Appl. Polym. Sci. Symp. 66 (1997) 1721–1729.
[7] D.A. da Silva, R.C.M. de Paula, J.P.A. Feitosa, Graft copolymerisation of acrylamide onto cashew gum, Eur. Polym. J. 43 (2007) 2620–2628.
[8] A. Hebeish, I. AbdEl-Thalouth, M.A. El-Kashouti, S.H. Abdel-Fattah, Graft copolymerization of acrylonitrile onto starch using potassium permanganate as initiator, Die Angew. Makromol. Chem. 78 (2003) 101–108.
[9] Z.L. Xu, Y.H. Yang, Y.M. Jiang, Y.M. Sun, Y.D. Shen, J. Pang, Synthesis and characterization of konjac glucomannan-graft-polyacrylamide via gamma-irradiation, Molecules 13 (2008) 490–500.
[10] Y.Q. Zhang, B.J. Xie, X. Gan, Advance in the applications of konjac glucomannan and its derivatives, Carbohydr. Polym. 60 (2005) 27–31.
[11] D.T. Tian, X. Wu, C.M. Liu, H.Q. Xie, Synthesis and flocculation behavior of cationic Konjac glucomannan containing quaternary ammonium substituents, J. Appl. Polym. Sci. 115 (2010) 2368–2374.
[12] J.C. Duan, Q. Liu, R.W. Chen, Y.Q. Duan, L.F. Wang, L. Gao, S.Y. Pan, Synthesis of a novel flocculant on the basis of crosslinked Konjac glucomannan-graft-polyacrylamide-co-sodium xanthate and its application in removal of Cu^{2+} ion, Carbohydr. Polym. 80 (2010) 436–441.
[13] C.X. Xie, Y.J. Feng, W.P. Cao, Y. Xia, Z.Y. Lu, Novel biodegradable flocculating agents prepared by phosphate modification of Konjac, Carbohydr. Polym. 67 (2007) 566–571.
[14] K. Katsuraya, K. Okuyama, K. Hatanakab, R. Oshimab, T. Satoc, K. Matsuzaki, Constitution of Konjac glucomannan: chemical analysis and C-13 NMR spectroscopy, Carbohydr. Polym. 53 (2003) 183–189.
[15] K. Kato, K. Matsuda, Studies on the chemical structure of Konjac mannan. Part I. Isolation and characterization of oligosaccharides from the partial acid hydrolyzate of the mannan, Agric. Biol. Chem. 33 (1969) 1446–1453.
[16] FMC Corp., Nutricol-Konjac General Technology Bulletin, Food Ingredients Division, 1993.
[17] A. Li, R. Liu, A. Wang, Preparation of starch-graft-poly(acrylamide)/attapulgite superabsorbent composite, J. Appl. Polym. Sci. Symp. 98 (2005) 1351–1357.
[18] H. Yu, Y. Huang, H. Ying, Preparation and characterization of a quaternary ammonium derivative of Konjac glucomannan, Carbohydr. Polym. 69 (2007) 29–40.
[19] J. Lu, C.B. Xiao, Preparation and characterization of carboxymethyl Konjac glucomannan/sodium montmorillonite hybrid films, J. Appl. Polym. Sci. Symp. 103 (2007) 2954–2961.
[20] B. Li, J.F. Kennedy, Q.G. Jiang, B.J. Xie, Single molecular chain geometry of Konjac glucomannan as a high quality dietary fiber in East Asia, Food Res. Int. 39 (2006) 127–132.
[21] C.X. Xie, Y.J. Feng, W.P. Cao, Novel biodegradable flocculating agents prepared by phosphate modification of Konjac, Carbohydr. Polym. 67 (2007) 566–571.
[22] M.B. Hocking, K.A. Klimchuk, S. Lowen, Polymeric flocculants and flocculation, Polym. Rev. 39 (1999) 177–203.
[23] F. Delval, L. Janus, J. Vebrel, M. Morcellet, G. Crini, Novel crosslinked gels with starch derivatives. Polymer–water interactions. Applications in waste water treatment, Macromol. Symp. 166 (2001) 103–108.
[24] F. Delval, G. Crini, J. Vebrel, M. Knorr, G. Sauvin, E. Conte, Starch-modified filters used for the removal of dyes from waste water, Macromol. Symp. 203 (2003) 1022–1360.
[25] J.G. Chen, C.H. Liu, Y.Q. Chen, Y. Chen, P.R. Chang, Structural characterization and properties of starch/Konjac glucomannan blend films, Carbohydr. Polym. 74 (2008) 946–952.
[26] H.Q. Yu, A.B. Huang, C.B. Xiao, Characteristics of Konjac glucomannan and poly (acrylic acid) blend films for controlled drug release, J. Appl. Polym. Sci. Symp. 100 (2006) 1561–1570.
[27] S. Mishra, R. Bajpai, R. Katare, A.K. Bajpai, Preparation, characterization and microhardness study of semi-interpenetrating polymer networks of polyvinyl alcohol and crosslinked polyacrylamide, J. Mater. Sci. Mater. Med. 17 (2006) 1305–1313.
[28] K.S Soppirnath, T.M. Aminabhavi, Water transport and drug release study from cross-linked polyacrylamide grafted guar gum hydrogel microspheres for the controlled release application, Eur. J. Pharm. Biopharm. 53 (2002) 87–98.
[29] J.A. Dean, Lang's Handbook of Chemistry, 15th ed., Mcgraw-Hill, New York, 1999.
[30] B. Zhang, R.Y. Yang, Y. Zhao, C.Z. Liu, Separation of chlorogenic acid from honeysuckle crude extracts by macroporous resins, J. Chromatogr. B: Biomed. Sci. Appl. 867 (2008) 253–258.
[31] C.X. Liu, R.B. Bai, Adsorptive removal of copper ions with highly porous chitosan/cellulose acetate blend hollow fiber membranes, J. Membr. Sci. 284 (2006) 313–322.
[32] P. Ding, K.L. Huang, G.Y. Li, Y.F. Liu, W.W. Zeng, Kinetics of adsorption of Zn (II) ion on chitosan derivatives, Int. J. Biol. Macromol. 39 (2006) 222–227.